

## Hydrogenated amorphous carbon film coating of PET bottles for gas diffusion barriers

Naima Boutroy<sup>a,\*</sup>, Yann Pernel<sup>a</sup>, J.M. Rius<sup>a</sup>, Florence Auger<sup>a</sup>, H.J.von Bardeleben<sup>b</sup>, J.L. Cantin<sup>b</sup>, F. Abel<sup>b</sup>, Andreas Zeinert<sup>c</sup>, C. Casiraghi<sup>d</sup>, A.C. Ferrari<sup>d</sup>, J. Robertson<sup>d</sup>

<sup>a</sup> Sidel, Le Havre, France

<sup>b</sup> INSP, Universités Paris 6 and 7, UMR 7588, Paris, France

<sup>c</sup> Université de Picardie LPMC Amiens, France

<sup>d</sup> Cambridge University, UK

Available online 2 February 2006

### Abstract

The addition of a gas-impermeable coating on the inside wall of a standard polyethylene terephthalate (PET) bottle has long been considered as a way to improve the packaging for beer, juice and carbonated soft drinks. We have developed a plasma-assisted deposition process suitable for the deposition of 100 nm thick, transparent, hydrogenated amorphous carbon (a-C:H) films on PET surfaces. The Sidel plasma technology uses an acetylene gas precursor and a microwave plasma, which allows us to obtain a high deposition rate of 60 nm/s necessary for industrial process flows. The a-C:H films provide a 50-fold reduction of the permeation rates of O<sub>2</sub>. The composition, optical, structural and defect properties of the a-C:H films were characterized by Rutherford Back Scattering (RBS), Elastic Recoil Detection Analysis (ERDA), X-ray Photoelectron Spectroscopy (XPS), optical spectroscopy, Raman and Electron Paramagnetic Resonance (EPR).

© 2005 Elsevier B.V. All rights reserved.

**Keywords:** Diamond-like carbon; Gas permeation; Structure; Optical gap

### 1. Introduction

Polyethylene terephthalate (PET) is a very valuable plastic that can be blown into containers and bottles. However, PET has a finite gas permeability that can limit the shelf life of some food and drink products. Diamond-like carbon (DLC) has a high atomic density [1] which has long been recognised and can be used as a gas permeation barrier [2,7–9]. A low permeability requires a large atomic density. In addition, the optical band gap of diamond-like carbon can be varied over a wide range [1], so that it could be possible to form an optically transparent gas permeation barrier. In addition, the a-C:H films must be deposited at a high rate to make a viable industrial process, but without exerting a large heat load which would

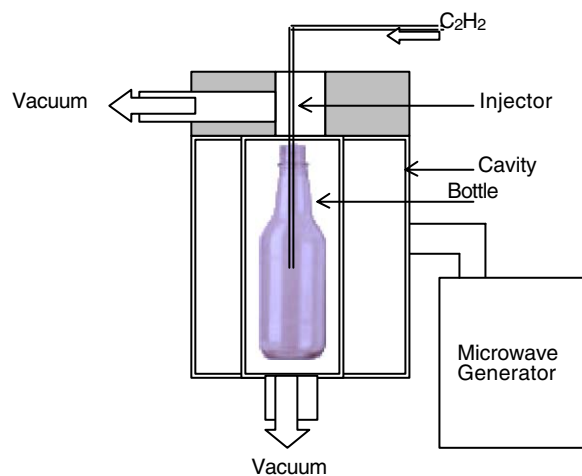


Fig. 1. Microwave plasma reactor.

\* Corresponding author. Sidel Group, Blowing & Coating Division, Avenue de la Patrouille de France, Octeville sur mer 76053, Le Havre Cedex, France. Tel.: +33 2 32 85 91 44; fax: +33 2 32 85 81 63.

E-mail address: [naima.boutroy@sidel.com](mailto:naima.boutroy@sidel.com) (N. Boutroy).

Table 1  
Process conditions

Microwave Power	Pressure	Gas	Gas flow rate	Deposition time
350 W	0.1 mbar	C <sub>2</sub> H <sub>2</sub>	160 sccm	3 s

Table 2  
Comparison of properties of a-C:H prepared from different process gases

Gas	Deposition rate	Oxygen transmission rate	BIF <sup>a</sup>
C <sub>2</sub> H <sub>2</sub>	60 nm/s	0.002 cc/Package/24 H	20
CH <sub>4</sub>	4 nm/s	0.030 cc/Package/24 H	1.3
C <sub>2</sub> H <sub>4</sub>	25 nm/s	0.012 cc/Pckage/24 H	3.3

<sup>a</sup> BIF: Barrier Improvement Factor is the ratio of a non-coated bottle to a coated bottle.

soften the PET substrate. This paper describes the development of a plasma technology for the formation of transparent a-C:H films on the inside of PET bottles, their gas barrier properties, and the characterisation of the resulting films by various techniques.

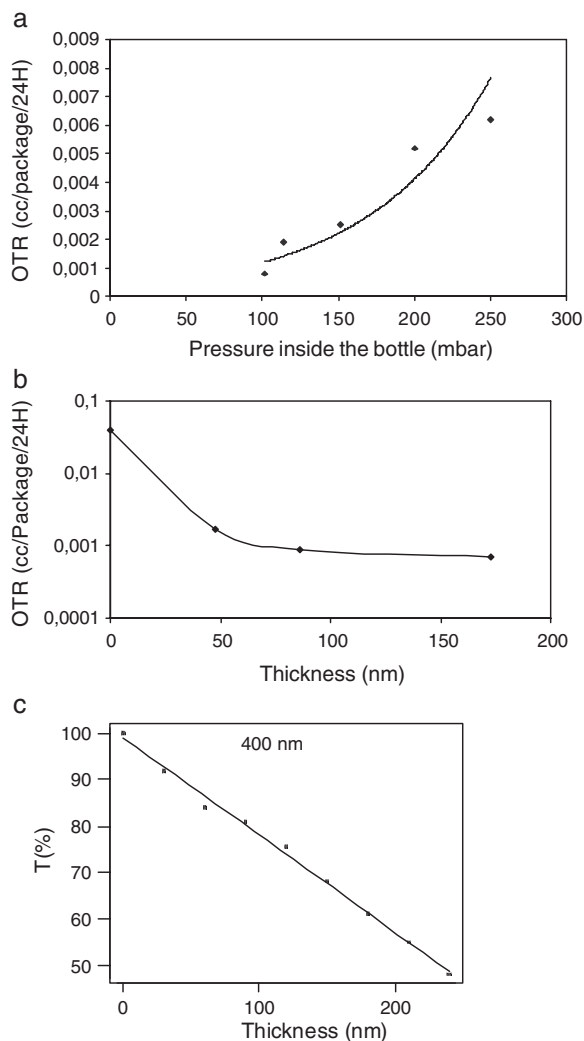


Fig. 2. (a) Oxygen transmission rate vs. process pressure inside the bottle. (b) Oxygen transmission rate vs. film thickness. (c) Optical transmission at 400 nm versus coating thickness.

## 2. Deposition

Hydrogenated amorphous carbon films were deposited inside a PET bottle in a microwave plasma reactor [3], as shown in the schematic of the equipment in Fig. 1. The bottle is placed neck-up inside the reactor. The pumping system creates a vacuum pressure of 50 mbar outside the bottle. At the same time, the inside of the bottle is pumped down to a pressure of around 0.1 mbar. This pressure difference between inside and outside prevents the bottle from collapsing. An open-ended tube is introduced inside the bottle to inject the acetylene process gas at a flow rate of 100–200 sccm. A 2.45 GHz microwave discharge is ignited for 1–3 s at a power of 200–

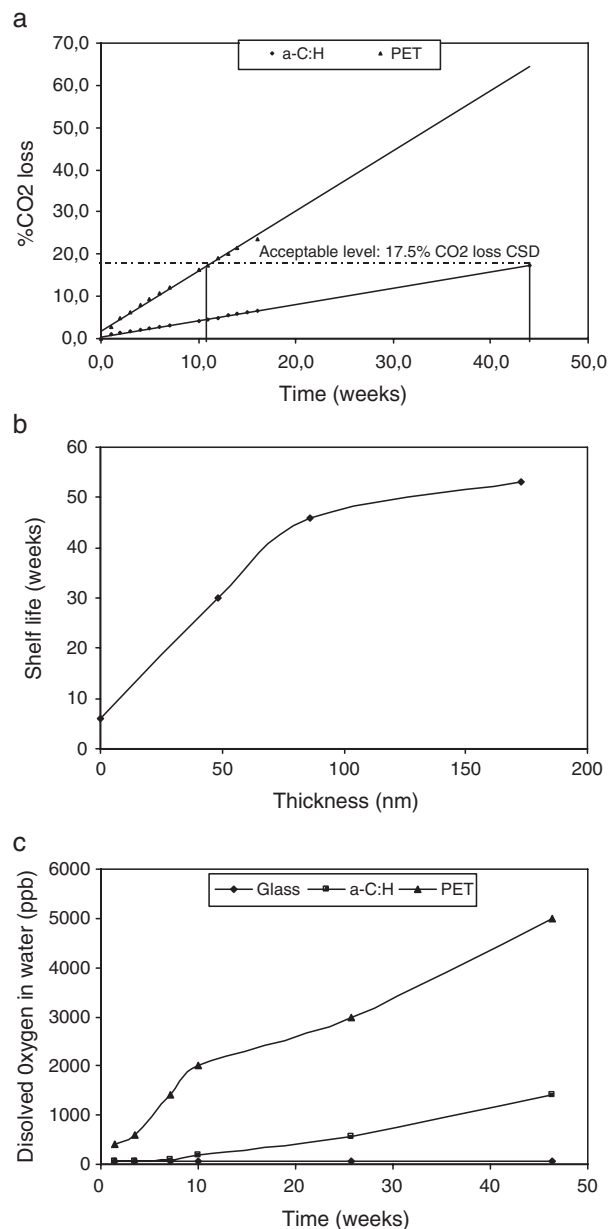


Fig. 3. (a) CO<sub>2</sub> loss of a 100 nm coated and a non-coated PET bottle versus storage time. (b) PET container shelf life vs. thickness of the coating. (c) Dissolved oxygen in water versus time of a PET bottle coated and non-coated compared to a glass bottle.

500 W to deposit the films. The process conditions are summarised in Table 1. The gas barrier transmission rates were measured using a Mocon Oxtran system.

The process conditions must satisfy three constraints; give a dense film which acts as a gas permeation barrier, a transparent film, not excessive heat load on the PET, and a rapid deposition rate for a viable industrial process. These are stringent and conflicting constraints. The requirement for a dense film generally conflicts with the need for transparency and a wide optical gap. Typical a-C:H films have a gap of 1–2 eV. a-C:H films have a wider gap if they are deposited with a large hydrogen content and large  $sp^3$  content. However, these films have a lower density.

The film thickness was measured on different areas of the PET bottle using a Dektak 3 profilometer. The film thickness is found to be uniform within  $\pm 15\%$  over the bottle interior. Ex-situ ellipsometry measurements give similar thickness values. The deposition rate is found to be 60 nm/s with acetylene as the process gas. This is extremely high compared to other processes such as capacitively coupled RF plasma deposition, which give rates of 0.1–1 nm/s [1]. The high rate indicates the extremely dense plasma created by the microwave discharge.

Using acetylene as process gas gives a faster deposition rate than other gases such as methane or ethylene. This is clear from Table 2 which compares the deposition rate, oxygen permeation rate and barrier improvement factor of films made from these three gases. Acetylene is well known to give one of the fastest deposition rates of any hydrocarbon. A faster deposition rate also reduces the deposition time for a given film thickness, and thus the total heat load on the PET.

The process conditions are then optimized for the precise operating pressure, microwave power and film thickness. These process parameters are summarized in the Table 1.

### 3. Barrier performances

The total cycle time from loading the bottle inside the coating machine to ejecting it from the machine is 7.2 s [4,5]. The process time including the coating and the pumping is 3.5 s

Table 3  
Simulation data for the RBS and ERDA spectra

Layer	Composition	Thickness ( $10^{15}$ atoms/cm $^2$ )	Comment
1	C (graphite)	100	Surface layer
2	$C_1H_{0.7}O_{0.06}$	1700	a-C:H layer
3	$C_{10}H_3O_{0.35}$	500	Modified PET
4	$C_{10}H_8O_4$	> 11 000	PET

The simulation is done with 4 layers: graphite cap layer (1), a-C:H layer (2), modified PET (3) and PET (4). Layer thickness is given in  $10^{15}$  atoms/cm $^2$ .

[4,5]. The real challenge in this machinery is to prevent leaks to reach the pressure needed for the process to guarantee the same quality of the coating during the production of 10,000 bottles/h. The effect of the process pressure was studied on the barrier performances of the a-C:H coating. Fig. 2(a) shows that the oxygen permeation rate reduces as the process pressure reduces. Lower process pressures lead to higher degrees of gas dissociation and ionization in the plasma during deposition, an increase in film density and diamond-like character and some reduction in band gap. Lower process pressures also lead to less incorporation of oxygen during the deposition process. The presence of oxygen in the coating structure gives a low density coating with worse gas barrier performance.

The process conditions are then optimized for the precise operating pressure, microwave power, and gas flow rate for a deposition time not higher than 3 s. These process parameters are summarized on the Table 1.

The gas permeation rate measured by the Mocon machines show that the permeation rate is reduced from 0.04 cm $^3$ /package/24 h for a plain PET bottle to 0.0008 cm $^3$ /package/24 h for a 100 nm a-C:H coated bottle. Fig. 2(b) plots the oxygen transmission rate versus the coating thickness using the process parameters described on the Table 1. It shows that the majority of the decrease in permeation rate occurs by 40 nm thickness. Greater thickness does not decrease the permeation rate proportionately. The thickness then is chosen depending on the application.

Beer application needs the highest oxygen barrier improvement meaning the thickest coating, 150 nm. The juice and carbonated soft drinks need a medium gas barrier improve-

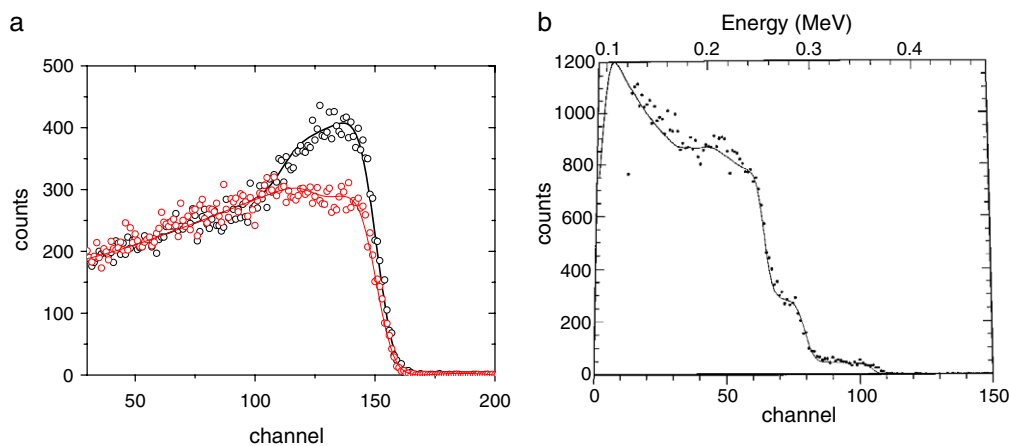


Fig. 4. (a) ERDA spectra of the DLC/PET stack (black) and a PET reference layer (red), experimental results (points), fit (line). (b) RBS spectrum of the DLC/PET stack (black), experimental results (points), fit (line). (For interpretation of the references to colour in this figure legend, the reader is referred to the web version of this article.)

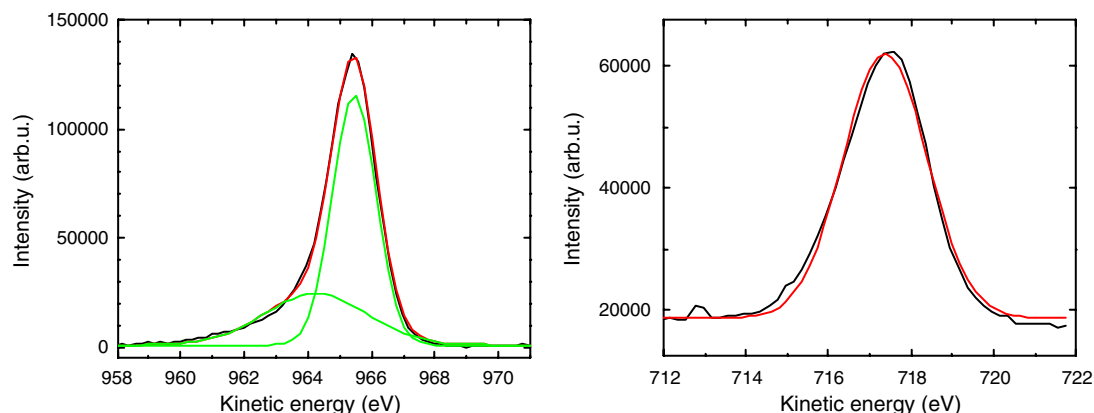


Fig. 5. (a) XPS spectrum of the 1s C emission; the total spectrum (red) is decomposed in two peaks: C–C and C–O. (b) XPS spectrum of the 1s O emission. (For interpretation of the references to colour in this figure legend, the reader is referred to the web version of this article.)

ment, a thickness between 40 and 60 nm gives good performances. The juice and the carbonated soft drinks markets are concerned about the transparency of the a-C:H coating because most of their containers are transparent and also some countries like Japan are concerned with the recyclability of the package. The optical transmission of this coating was measured using a UV/Vis spectrometer, and is shown in the Fig. 2(c) for different coating thickness. The optical transmission is 80% at 400 nm and 97% at 700 nm. The compromise between permeability and optical gap has been resolved so that the DLC film is sufficiently transparent. It does, however, retain a brown tint due to the wide absorption edge. A more transparent film can be obtained at the expense of higher permeability, by either making a wider gap or a thinner film. The resulting process requirements are reasonably similar to those for protective coatings on future optical storage disks [6].

Fig. 3(a) plots the CO<sub>2</sub> loss of a coated and a non-coated PET container versus storage time at 21 °C. The shelf-life is then extrapolated from this curve for 17.5% loss of CO<sub>2</sub> for soft drinks beverages and for 10% loss of CO<sub>2</sub> for beer applications. A uncoated container has 10 weeks shelf-life and a coated container has 44–45 week shelf-life for soft drinks and for beer a non-coated container has just 4 weeks and a coated container has 38 weeks shelf-life. These performances can be improved by increasing the thickness of the coating, as shown on Fig. 3(b).

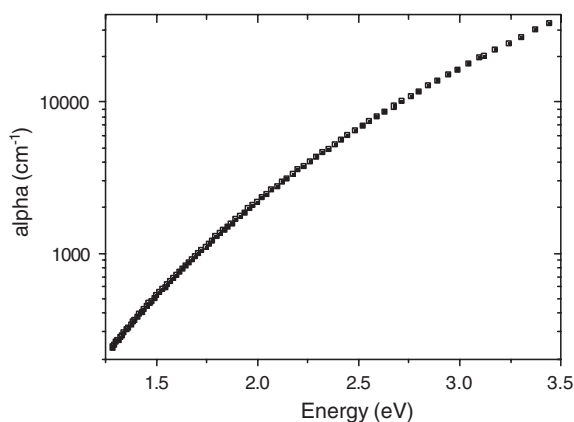


Fig. 6. Optical absorption coefficient as a function of energy.

The CO<sub>2</sub> loss during storage time is not the only important factor to preserve the good taste of beer. Keeping the beer from oxidation is also an important factor. 1000 ppb of dissolved oxygen is the maximum quantity acceptable for beer, 50% of it comes from the head space, during the filling, and from the oxygen in beer before filling, and the other 50% is related to the package. The latter was measured during the storage time at

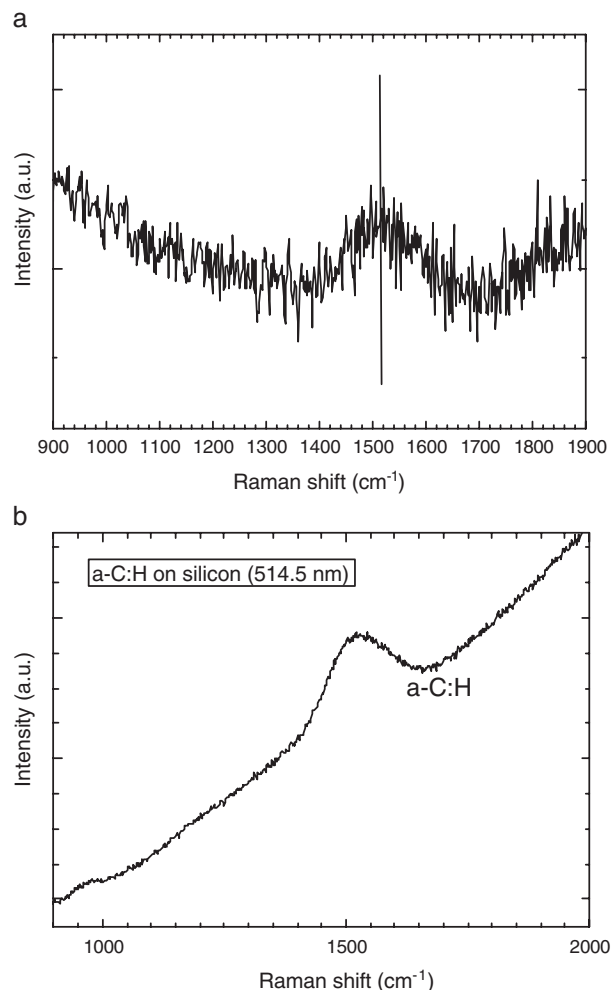


Fig. 7. Raman spectrum at 514 nm excitation of the a-C:H on (a) PET substrate, (b) a Si substrate.

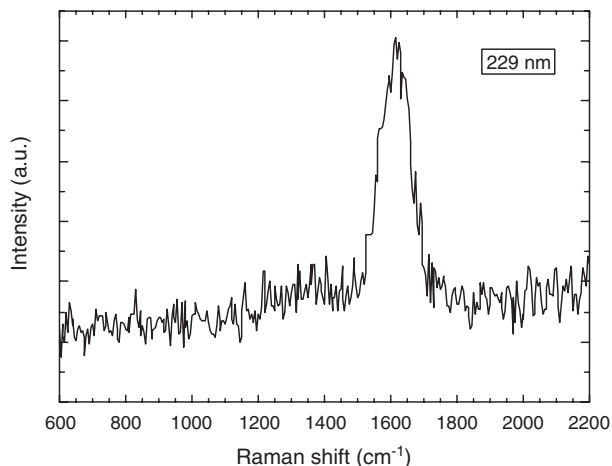


Fig. 8. Raman spectrum excitation at 229 nm for the a-C:H on a PET substrate.

21 °C, shown on Fig. 3(c). It shows a shelf-life around 25 weeks for a coated PET container and 3 weeks for a non-coated PET bottle. These results were obtained with a 100-nm-thick coating.

#### 4. Elemental analysis

The resulting films were characterized in terms of their chemical composition, optical properties and structural properties. The total composition of the a-C:H layers deposited on PET was determined by standard Rutherford Backscattering Spectroscopy (RBS) and Elastic Recoil Detection Analysis (ERDA). Both experiments were performed with 2 MeV <sup>4</sup>He ions. Care was taken to avoid sample degradation under the analyzing beam. The collected charge did not exceed 10 μC and to avoid charge build-up a 10-nm-thin conductive graphite layer was deposited on the DLC layer. The RBS and ERDA spectra were analyzed using the RUMP program. The analysis depth of these techniques is of the order of 1 μm. As the DLC is only 0.2 μm thick, this allows us also to probe the composition of the underlying PET layer. XPS measurements

were carried out with non-monochromatic Mg source and the 1s C and 1s O peaks were analysed. With XPS, being a surface technique, only the 3 nm surface layer of the a-C:H film is analysed.

Fig. 4(a) and (b) show the EDRA and RBS spectra of the a-C:H/PET stack. We have equally superposed in Fig. 4(a) the ERDA spectrum of a PET reference sample. The large hydrogen content in the DLC film gives rise to the well-resolved peak structure between channels 100 and 150. Both spectra were simulated with the same set of parameters. It was not possible to fit these data with a simple model of a-C:H layer and a PET substrate with a homogenous stoichiometric composition of C<sub>10</sub>H<sub>8</sub>O<sub>4</sub>. A modified PET interface layer must be included to get a good fit (Table 3). Taking a DLC layer of uniform composition C<sub>1</sub>H<sub>x</sub>O<sub>y</sub>, we deduce x=0.70 and y=0.06. Thus, the DLC film is very hydrogen rich and partially oxidized. The areal atomic density of DLC found by RBS corresponds to a mass density of 1.3 g/cm<sup>3</sup>.

The RBS profile indicates that the oxidation is not limited to the surface layer but is homogenous in the entire film thickness. For the PET, we must include an intermediate layer of a modified composition. This layer 3 (Table 3) has a thickness of 500 × 10<sup>15</sup> cm<sup>-2</sup> atoms and a composition of C<sub>10</sub>H<sub>3</sub>O<sub>3.5</sub>, compared to the normal PET composition of C<sub>10</sub>H<sub>8</sub>O<sub>4</sub>. Thus the interface region, which is crucial for the adhesion of the DLC layer to its PET substrate, is characterized by a much lower H content and a somewhat lower O content. This indicates that the microwave plasma achieves a good adhesion by plasma etching of the underlying PET.

Fig. 5 shows the XPS results. The C 1s spectrum shows an asymmetric lineshape. The spectrum can be simulated by the sum of two Gaussian peaks. The parameters of the fit are given in the figures. The high energy component (C2) has a linewidth of 1.4 eV and has 2/3 of the total intensity. The second component (C1) is much wider, 3.2 eV, and has a binding energy of 1.2 eV less than the peak C2. The peak positions change in the same way as the O1s spectra with the detection angle. For normal incidence, the peak C1 is at 964.2 eV and C2

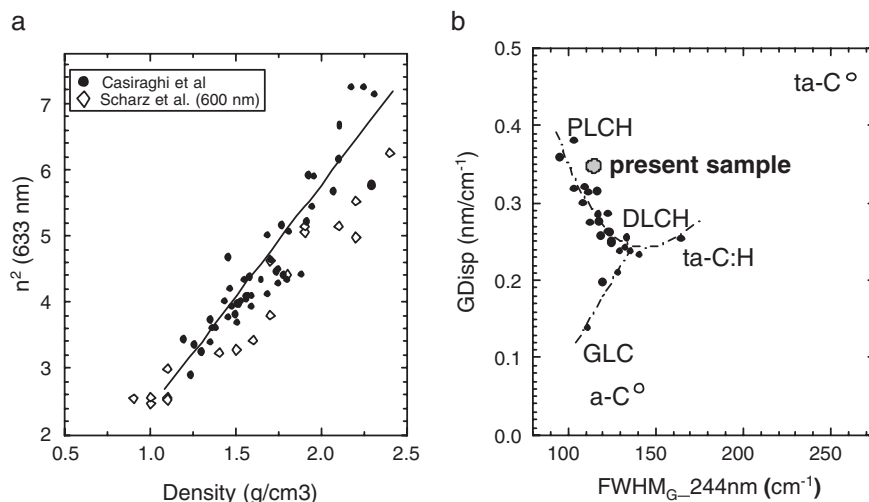


Fig. 9. (a) Correlation between the refractive index square and the density of a-C:H films deposited by different methods. (b) Correlation of the dispersion of the G peak in the Raman spectrum versus the width of the G peak in UV (244 nm) excitation, can be used to classify the various types of diamond-like carbon.

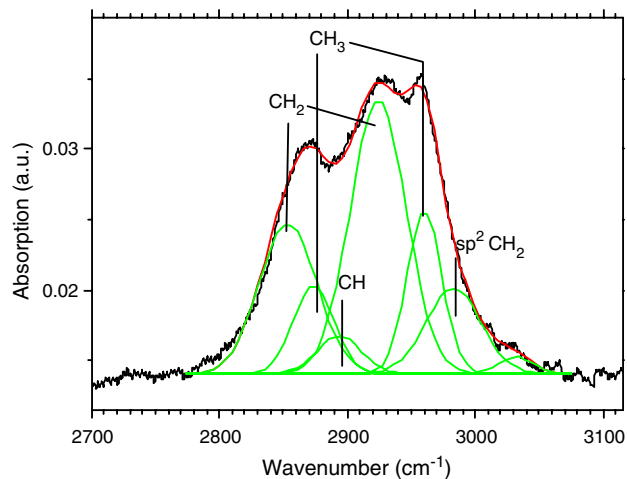


Fig. 10. Infra-red absorption spectrum of a-C:H layer.

at 965.5 eV and change for 65° detection to 965.5 and 966.7 eV. The energy position and the difference in the binding energy allows us to attribute the dominant peak (C2) to C–C bonds and the second peak to C–O bonds. The O1s spectrum in Fig. 5 is characterized by a single peak with a symmetric lineshape which we have fitted with a Gaussian lineshape and a broad baseline. For detection normal to the surface, the O1s peak lies at a binding energy of 536.1 eV.

## 5. Structural analysis

The optical constants of the a-C:H films deposited on PET were determined in the spectral range going from 1 eV to 3.5 eV by a combination of transmittance and reflectance spectroscopy using a Cary 5E spectrophotometer. The analysis of the spectra was performed with a commercial FilmWizard programme using different dispersion models. The optical properties of the PET substrate were investigated separately in order to get an accurate fit of the experimental data. The optical constants of the PET are found to be similar to recent literature data [10]. For a higher precision fit, the film thickness was checked independently with a Dektak 3 profilometer. The optical gap E04 of the a-C:H films in Fig. 6 is found to be 2.7 eV while the refractive index is about 1.8 at 600 nm in accordance with spectroscopy ellipsometry measurements. The optical spectrum has a long absorption tail.

The Raman spectra of the DLC films were measured for films deposited on both PET and Si substrates for both 514 nm and at 229 nm (UV) excitation. The 514 nm spectrum is clearer for the film deposited on Si, but the spectrum for a-C:H on PET is the critical spectrum, as the Si wafer may disturb the plasma. The 514 nm spectra are shown in Fig. 7 after removal of some background due to PET. The main G peak of the DLC is found to lie at 1518 cm<sup>-1</sup>, corresponding to a polymeric DLC film. The peak is due to vibrations of C–C sp<sup>2</sup> bonds. The full width half maximum (FWHM) is 145 cm<sup>-1</sup>. There is no evidence of any D peak, indicating that there are few aromatic species present. The UV Raman spectra in Fig. 8 obtained on PET substrate show a G peak at 1619 cm<sup>-1</sup> with a FWHM of 118 cm<sup>-1</sup>. Thus, the G peak shifts with excitation wavelength, and its width reduces. The narrow peak at 1730 cm<sup>-1</sup> is due to the PET substrate.

We can analyze the structural properties of the DLC from the position and width of the G peak and from its dispersion with excitation wavelength [11]. For a wide variety of DLCs, we have found that the G peak width correlates with the DLC density, refractive index and Young's modulus, while the dispersion of the G wavenumber correlates with the sp<sup>3</sup> content and band gap. The G peak dispersion is derived to be 0.35 cm<sup>-1</sup>/nm. This corresponds to a sp<sup>3</sup> content of over 80%. The G peak wavenumber is also consistent with this high sp<sup>3</sup> content.

The G peak width is consistent with a density of order 1.4 g/cm<sup>3</sup>. The refractive index, *n*, of 1.8 is consistent with a density of 1.3 g/cm<sup>3</sup> from the known linear correlation of *n*<sup>2</sup> and density for DLC deposited on other systems [11], as shown in Fig. 9(a). A similar density of 1.3 g/cm<sup>3</sup> is derived by RBS. The parameters derived from Raman allow us to place this a-C:H film amongst the different types of DLC as is seen in Fig. 9(b).

We can also extract a hydrogen content from the slope of the luminescence background of the 514 nm spectrum of the sample on Si [11]. The background varies exponentially with H content for a-C:H. We find *x*=67% H, when expressed as a-CH<sub>*x*</sub>, similar to that found by ERDA.

Fig. 10 shows the infra-red absorption spectrum of the a-C:H in the 2800–3200 cm<sup>-1</sup> range, which is due to C–H bond stretching modes. This can be analyzed to give a rough indication of the different CH<sub>*n*</sub> groups present. We use the

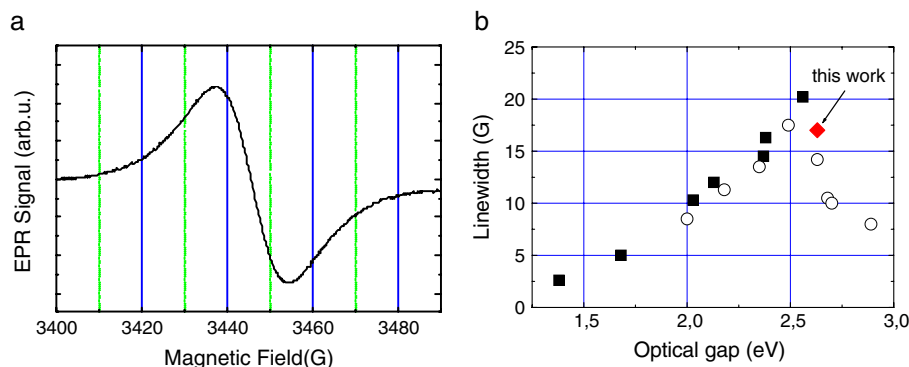


Fig. 11. (a) X-band EPR spectrum of the a-C:H layer; *T*=300 K. (b) Comparison of X-band EPR linewidths in a-C:H and a-C layers after Ref. [13] and our work (◊).

assignments and oscillator strengths of Ristein et al. [12], giving  $\equiv\text{CH}:\text{=CH}_2:-\text{CH}_3=0.06:0.73:0.20$  for the predominant  $\text{sp}^3$  carbon sites.

Fig. 11(a) shows the room temperature EPR spectrum of this a-C:H layer. The PET substrate does not contribute to the EPR spectrum. The EPR spectrum consists of a single symmetric line of Lorentzian lineshape, a  $g$ -value of 2.0030 and a spin density of  $1.5 \times 10^{20}$  spins/cm<sup>3</sup>. The peak-to-peak linewidth is 16.2 G, one of the largest linewidths ever found for a-C:H (Fig. 11(b)). The exceptional width of 16.2 G arises from the dipolar broadening by hydrogen, which is consistent with the very high H content [13]. It is typical for a high gap material with  $E_{04}=2.7$  eV (Fig. 11), a value in good agreement with the measured optical transmission spectrum.

## 6. Conclusion

We have shown that by combining acetylene gas precursor and a microwave plasma it is possible to obtain a high deposition rate with a wide choice of deposition parameters.

The thin a-C:H coatings obtained have an exceptional structural properties characterized by a high hydrogen content, a high  $\text{sp}^3$  fraction, and a high optical transparency, combining good adhesion properties on PET with an efficient gas diffusion barrier.

The a-C:H coating using acetylene gas as a precursor is well placed as an industrial barrier coating in the packaging industry compared to  $\text{SiO}_x$  coating. The  $\text{SiO}_x$  coating has an advantage of its transparency but the process window for PECVD is so small that it makes it impossible to guarantee a reliable process, while the a-C:H coating has a very large process window as discussed in this paper.

## References

- [1] J. Robertson, *Mater. Sci. Eng.*, R Rep. 37 (2002) 129.
- [2] C. Wild, P. Koidl, *App. Phys. Lett.* 51 (1987) 1506.
- [3] EP 1 198 611.
- [4] US 6,827,972.
- [5] US 6,818,068.
- [6] F. Piazza, D. Grambole, D. Schneider, S. Casiraghi, A.C. Ferrari, J. Robertson, *Diamond Relat. Mater.* 14 (2005) 994.
- [7] G.A. Abbas, S.S. Roy, P. Papakonstantinou, J.A. McLaughlin, *Carbon* 43 (2005) 303.
- [8] M. Yoshida, T. Tanaka, S. Watanabe, M. Shinohara, J.W. Lee, T. Takagi, *Surf. Coat. Technol.* 174–175 (2003) 1033.
- [9] S. Yamamoto, H. Kodama, T. Hasebe, A. Shirakura, T. Suzuki, *Diamond Relat. Mater.* 14 (2005) 1112.
- [10] S. Logothetidis, M. Gioti, C. Gravalidis, *Synth. Met.* 138 (2003) 369.
- [11] C. Casiraghi, A.C. Ferrari, J. Robertson, *Phys. Rev.*, B 72 (2005) 085401.
- [12] J. Ristein, R.T. Stief, L. Ley, W. Beyer, *J. Appl. Phys.* 84 (1998) 3836.
- [13] R.C. Barklie, *Diamond Relat. Mater.* 10 (2001) 174.